arXiv:2610.24458v1 [cs.LG] 17 Oct 2026

Generative Retrieval for Reverse Target Fishing with a Proteome-Scale Benchmark

Zhichao Deng[1,2,3,*,‡], Haichuan Tan[1,2,4,*], Xin Hong[2], Huaizhi Wang[1,2,3], Tao Huang[1,2,3], Bowen Gao[1,2,4], Yanyan Lan[1,2,†]

[1]AIPher Technology

[2]Institute for AI Industry Research (AIR), Tsinghua University

[3]School of Pharmaceutical Sciences, Peking University

[4]Department of Computer Science and Technology, Tsinghua University

Zhichao Deng: 2310307113@stu.pku.edu.cn

[*]These authors contributed equally to this work.

[†]Corresponding author: lanyanyan@air.tsinghua.edu.cn

[‡]Work done during an internship at AIPher Technology.

Abstract

Reverse target fishing identifies protein targets for a query molecule and is central to drug discovery and repurposing. Discriminative approaches adapted from virtual screening face sparse, long-tailed associations and missing-not-at-random measurements: treating unrecorded pairs as negatives can suppress genuine targets. We reformulate the task as generative retrieval and introduce **GenFish**. Residual vector quantization converts frozen protein language model features into shared semantic identifiers. Given a molecular fingerprint, GenFish autoregressively models codes conditioned on the query and preceding code, ranking proteins by identifier likelihood without explicitly labeling unrecorded pairs as negatives. We introduce **ProTargetBench**, the first proteome-scale benchmark for reverse target fishing to jointly support measured-panel discrimination and full-catalogue recovery of experimentally recorded positives. Covering 20,431 UniProt-reviewed human proteins, it integrates curated bioactivity evidence and distinguishes experimental inactivity from unmeasured associations. On 198 held-out molecules, GenFish achieves higher mean performance across all three full-catalogue retrieval metrics than four discriminative neural baselines and three non-neural baselines, including ligand-based methods. A controlled positive-hiding experiment shows that targeted removal of false-negative competition improves contrastive retrieval beyond matched random masking; GenFish remains stronger under the same incomplete supervision. Pfam alignment indicates that the semantic identifiers capture biologically meaningful relationships among proteins. These results establish generative retrieval as a principled paradigm for reverse target fishing under incomplete bioactivity records.

1 Introduction

Reverse target fishing asks which proteins in the human body a small molecule may bind to or affect. Identifying these proteins can help us understand how a drug works, detect unintended interactions, and discover new uses for existing compounds [3, 8]. Unlike conventional virtual screening, which fixes a protein and searches for molecules, reverse target fishing fixes the molecule and searches over a large protein catalogue. The task is therefore to rank many possible protein targets for each

molecule.

A central difficulty is that bioactivity databases record molecule–protein associations selectively. An observed pair can provide positive activity evidence, whereas an unrecorded pair may simply not have been measured. This distinction is especially important because assays focus on selected proteins, leaving individual molecules sparsely annotated and targets unevenly studied. Our training data contain 381,225 positive associations for 291,337 molecules, or only about 1.3 recorded targets per molecule on average. Treating all unrecorded pairs as negative samples or contrastive competitors can therefore suppress genuine but undiscovered targets, as illustrated in Figure 1.

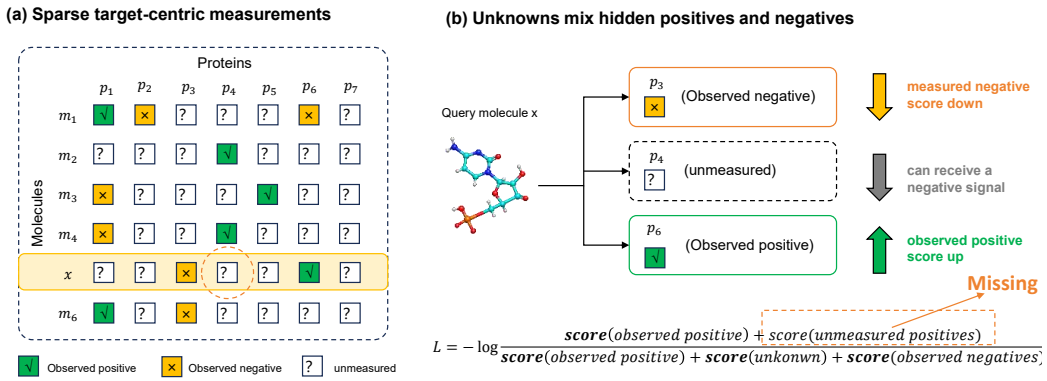


Figure 1: **Why sparse reverse target-fishing supervision is difficult.** Unmeasured molecule–protein pairs may include both hidden binders and non-binders; treating candidate-level unknowns as negative competitors can suppress undiscovered targets.

This asymmetry raises a modelling question: can sparse positive associations share information across proteins without assigning unknown molecule–protein pairs negative labels? A useful representation should transfer supervision across related proteins while preserving distinctions between candidates. We address this question with **GenFish**: protein representations are quantized into shared, multi-level semantic identifiers, allowing observed associations to share supervision across candidates without explicitly treating unmeasured pairs as negatives [19, 21].

Specifically, GenFish uses residual vector quantization to construct semantic identifiers from frozen protein language-model features. Given a molecule, it autoregressively predicts the identifier codes and ranks the fixed protein catalogue by their likelihood, using molecule-conditioned transitions between successive semantic codes. This preserves molecule-specific preferences while sharing statistical strength across related proteins.

Evaluating this problem requires a benchmark that covers both capabilities. Existing evaluations either discriminate activity within selected assay panels or score candidates in a broad structural catalogue: the former lacks proteome-scale recovery, while the latter usually lacks curated supervision and does not distinguish experimental inactivity from unmeasured pairs. We therefore introduce **ProTargetBench**, which integrates curated associations from ChEMBL, BindingDB, and PubChem [9, 12, 15] with a fixed catalogue of 20,431 UniProt-reviewed human proteins. It evaluates measured-panel discrimination and full-catalogue recovery under the same candidate space while preserving the distinction between inactive and unmeasured pairs.

On 198 held-out molecules, GenFish achieves the highest mean performance among the evaluated neural and non-neural baselines on all three full-catalogue retrieval metrics. It reaches 35.27%

R@10, 51.96% R@50, and 46.31% MRR, including a 5.46-point R@50 improvement over the strongest neural comparator. A controlled positive-hiding experiment shows that removing false-negative competition improves contrastive retrieval, while GenFish remains stronger under the same incomplete supervision. Pfam analysis shows that the identifiers retain biologically meaningful structure.

Our contributions are:

- **Method:** We formulate reverse target fishing as retrieval over protein semantic identifiers and introduce **GenFish**, which learns from positive associations without explicitly treating unrecorded pairs as negatives.
- **Benchmark:** We introduce **ProTargetBench**, a proteome-scale benchmark spanning 20,431 UniProt-reviewed human proteins and separating measured-panel discrimination from full-catalogue positive recovery.
- **Evidence:** GenFish outperforms the evaluated neural and non-neural baselines on full-catalogue retrieval, while controlled experiments demonstrate the effect of false-negative competition and the contributions of the proposed identifier structure.

2 Related Work

Target fishing and molecular–protein retrieval. Reverse target-fishing methods include ligand-based similarity, structure-based reverse docking, and neural molecule–protein matching. SEA and SwissTargetPrediction transfer information from known active compounds [3, 7], while reverse docking and structure-aware models score candidate binding sites [10, 11]. Neural methods learn molecular and protein representations for interaction or affinity prediction, including contrastive retrieval models such as ConPLex and DrugCLIP and graph- or geometry-aware models such as LigUnity and HypSeek [4–6, 16, 17, 20, 22]. These approaches generally score molecule–protein pairs discriminatively, which can treat unmeasured pairs as negatives. Existing evaluations emphasize either measured-panel discrimination or broad structural candidate sets [1, 13, 14, 18, 24]; they do not combine a fixed proteome-scale catalogue with explicit positive, inactive, and unmeasured states. ProTargetBench addresses this gap by combining a fixed proteome-scale catalogue with measured-panel discrimination and full-catalogue recovery of recorded positives.

Generative retrieval and semantic identifiers. Generative retrieval models candidate identifiers conditioned on a query. DSI and TIGER established this paradigm for document retrieval and recommendation using semantic identifiers and residual quantization [19, 21]; LETTER studied related identifier structures [23]. GenFish adapts these ideas to protein retrieval by learning molecule-conditioned identifier likelihoods from observed positives.

3 Problem Formulation and GenFish

3.1 Problem Formulation

Let $\mathcal{X}$ denote the space of query molecules and let $\mathcal{P}$ be a fixed catalogue of candidate proteins. Given a query molecule $x \in \mathcal{X}$, reverse target fishing aims to rank proteins $p \in \mathcal{P}$ according to whether they may be affected by x. A molecule may have multiple relevant proteins, so the task is a multi-positive retrieval problem rather than single-label classification.

The available training data consist of observed positive associations

$$\mathcal{D}^+ = \{(x_i, p_i)\}_{i=1}^{N}.$$

An unrecorded pair $(x, p) \notin \mathcal{D}^+$ is unknown: it may correspond to a non-binder or to an interaction that has not been measured. We therefore do not define a complementary negative set over $\mathcal{X} \times \mathcal{P}$. Instead, the learning objective uses observed positive associations while leaving unrecorded pairs unlabeled.

The goal is to learn a query-dependent ranking function $s_\theta : \mathcal{X} \times \mathcal{P} \to \mathbb{R}$ and return

$$\mathrm{TopK}_\theta(x; \mathcal{P}) = \underset{S \subseteq \mathcal{P}\ |S|=K}{\arg\max} \sum_{p \in S} s_\theta(x, p).$$

The catalogue defines the search space, while the recorded positives define the known targets available for training and evaluation. GenFish is designed to mitigate sparse supervision by sharing statistical strength across protein identifiers without assigning unmeasured molecule–protein pairs negative labels.

3.2 GenFish Overview

GenFish represents each protein with a discrete semantic identifier derived from its sequence representation. The identifier is constructed from shared codebooks, allowing related proteins to share identifier components. A molecule-conditioned predictor then assigns likelihood to candidate identifiers. At inference, every catalogue protein is scored using its stored identifier, and candidates are ranked by identifier likelihood (Figure 2).

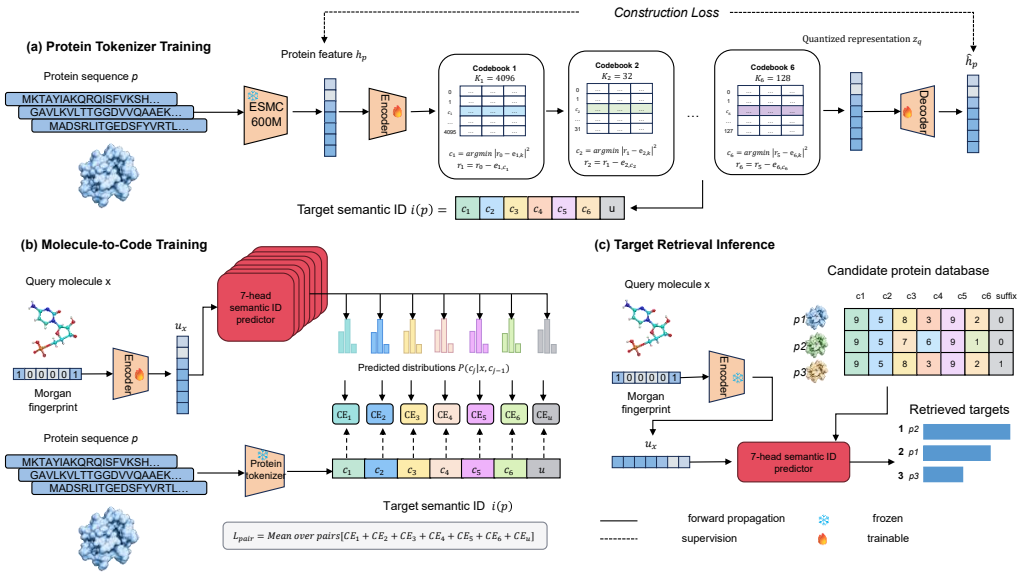


Figure 2: **Overview of GenFish.** (a) Protein tokenization: seven-component protein identifiers are constructed from quantized frozen ESMC-600M features. (b) Molecular prediction: observed positive associations train a molecular predictor to assign likelihoods to target identifiers from Morgan fingerprints. (c) Catalogue retrieval: candidate proteins are ranked by identifier likelihood, with each subsequent semantic code conditioned on the query molecule and the preceding code. Code values are illustrative and do not imply numerical similarity.

3.3 Protein Semantic Identifiers

We extract sequence features using frozen ESMC-600M and standardize them to obtain a protein representation $\mathbf{h}_p$. An encoder maps this representation into a low-dimensional latent space,

$$\mathbf{z}_p = E(\mathbf{h}_p).$$

Residual vector quantization converts the latent representation into a sequence of discrete codes. At each level, the nearest codebook vector is selected and subtracted from the remaining residual:

$$\mathbf{r}_0 = \mathbf{z}_p, \qquad c_j(p) = \arg\min_k \|\mathbf{r}_{j-1} - \mathbf{e}_{j,k}\|_2^2, \qquad \mathbf{r}_j = \mathbf{r}_{j-1} - \mathbf{e}_{j,c_j(p)}. \tag{1}$$

Here $\mathbf{e}_{j,k}$ denotes the k-th vector in the level-j codebook. A decoder reconstructs the protein features from the sum of the selected vectors. The encoder and codebooks are trained using reconstruction and quantization objectives, without molecule–protein interaction labels.

GenFish represents each protein with a seven-code identifier

$$\mathbf{c}(p) = \big(c_1(p), \ldots, c_6(p), c_7(p)\big).$$

Once tokenization is complete, all protein-side parameters and identifiers are frozen. Proteins that share code components also share the corresponding output parameters in the molecular predictor, allowing supervision from observed associations to propagate across related candidates.

3.4 Molecule-Conditioned Identifier Prediction

For a query molecule x, a multilayer perceptron maps its Morgan fingerprint to a query representation $\mathbf{u}_x$. The base logits at code level j are

$$\mathbf{a}_j(x) = W_j \mathbf{u}_x + \mathbf{b}_j.$$

For the intermediate levels $j = 2, \ldots, 6$, GenFish adds a low-rank interaction conditioned on the preceding code. Given preceding code a, the logit for current code k is

$$\ell_{j,k}(x, a) = a_{j,k}(x) + [\mathbf{g}_j(x) \odot \bar{\mathbf{U}}_j[a]]^\top \mathbf{V}_j[k], \qquad \mathbf{g}_j(x) = G_j \mathbf{u}_x + \mathbf{d}_j, \tag{2}$$

where $\bar{\mathbf{U}}_j[a]$ is the normalized embedding of the preceding code, $\mathbf{V}_j[k]$ is the current-code embedding, and $\odot$ denotes elementwise multiplication. The molecular gate allows the same preceding code to induce different predictions for different query molecules.

For the first and final code levels, the preceding-code interaction is omitted. Thus all seven code-level distributions can be written in the unified form

$$P_{\theta,j}(k \mid x, a) = \frac{\exp \ell_{j,k}(x, a)}{\sum_{v=0}^{K_j - 1} \exp \ell_{j,v}(x, a)}, \qquad j = 1, \ldots, 7, \tag{3}$$

where $a = c_{j-1}(p)$ for $j = 2, \ldots, 6$, while $a = \varnothing$ for $j = 1$ and $j = 7$. For $j = 1$ and $j = 7$, the resulting distribution depends only on x.

Let $c_0(p) = \varnothing$. The complete identifier likelihood is then

$$P_\theta(\mathbf{c}(p) \mid x) = \prod_{j=1}^{7} P_{\theta,j}(c_j(p) \mid x, c_{j-1}(p)). \tag{4}$$

This factorization shares parameters across proteins while allowing the query molecule to modulate the compatibility of successive identifier components.

3.5 Training and Catalogue Retrieval

Given the observed positive associations $\mathcal{D}^+$, GenFish minimizes the negative log-likelihood of the stored target identifiers:

$$\mathcal{L}(\theta) = -\frac{1}{|\mathcal{D}^+|} \sum_{(x,p)\in\mathcal{D}^+} \sum_{j=1}^{7} \log P_{\theta,j}(c_j(p) \mid x, c_{j-1}(p)) \,. \tag{5}$$

Each positive association contributes one training example. Multiple recorded targets for the same molecule therefore provide multi-positive supervision, while unrecorded molecule–protein pairs are not explicitly sampled as negative labels.

At inference, GenFish scores every candidate protein by the log-likelihood of its stored identifier:

$$s_\theta(x,p) = \log P_\theta(\mathbf{c}(p) \mid x) = \sum_{j=1}^{7} \log P_{\theta,j}(c_j(p) \mid x, c_{j-1}(p)) \,. \tag{6}$$

The catalogue proteins are ranked by this score and the highest-ranked candidates are returned. Because each candidate has a known valid identifier, its likelihood can be evaluated directly without unconstrained beam search. These scores represent the model's relative preference over target identifiers and are used for retrieval rather than interpreted as experimental binding probabilities.

4 ProTargetBench

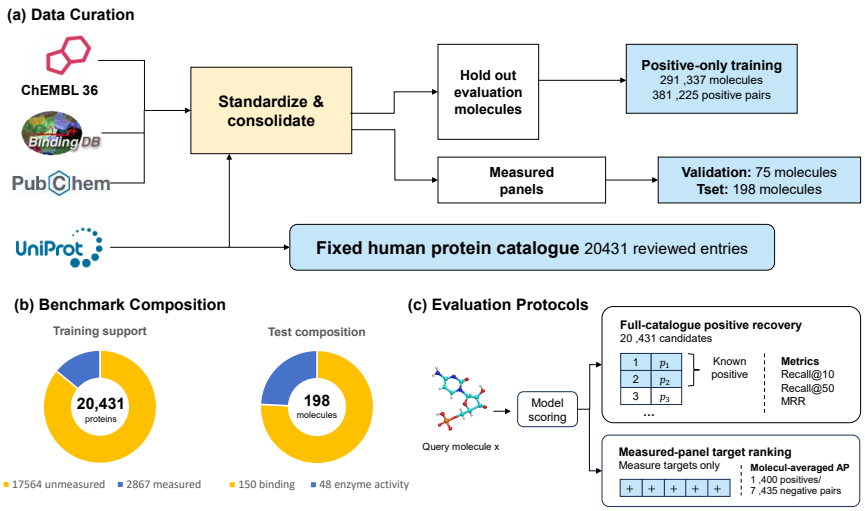


Figure 3: **ProTargetBench construction and evaluation.** The benchmark consolidates bioactivity evidence, fixes a human protein catalogue, and separates full-catalogue positive recovery from measured-panel target ranking.

ProTargetBench separates measured-panel discrimination from recovery of known positives in a fixed catalogue of 20,431 UniProt-reviewed human proteins, while preserving the distinction between experimental inactivity and unmeasured pairs.

4.1 Benchmark Construction

ProTargetBench integrates ChEMBL 36, BindingDB, and selected PubChem assays [9, 12, 15]. We standardize identities and retain eligible sub-micromolar K_i, K_d, and IC_{50} positives. Evaluation panels preserve source-specific positive and negative evidence; unmeasured pairs are not treated as inactive.

We provide fixed training, validation, and test partitions with scaffold and source-linked exclusions applied before aggregation. Full source versions, identity rules, label criteria, and exclusion procedures are documented in Appendix A.

4.2 Catalogue, Supervision, and Splits

The catalogue contains 20,431 proteins and training has 381,225 positive associations across 291,337 molecules. Validation and test sets contain 75 and 198 queries with 8,835 labeled test pairs.

Training-supported proteins form a subset of the catalogue, while measured test targets are defined only by held-out panels. The catalogue defines the search space; experimental records define supervision and evaluation labels. Catalogue coverage alone does not establish generalization to unsupported targets.

4.3 Evaluation Protocols

We evaluate the same model scores under two complementary protocols. Full-catalogue positive recovery evaluates whether a method can recover recorded positive targets from the entire protein catalogue. For each query molecule x, all 20,431 candidates are ranked against its recorded evaluation positives $\mathcal{R}_x$. We report Recall@10, Recall@50, and mean reciprocal rank (MRR), with

$$\mathrm{Recall@K}(x) = \frac{|\,\mathrm{TopK}_\theta(x;\mathcal{P}) \cap \mathcal{R}_x|}{|\mathcal{R}_x|}. \tag{7}$$

Reciprocal rank is computed from the highest-ranked known positive, and all retrieval metrics are averaged across query molecules. Unmeasured candidates remain unlabeled: the protocol assesses known-positive recovery rather than assigning experimental inactivity to the rest of the catalogue.

Measured-panel discrimination evaluates whether a method can distinguish active from inactive targets within the experimentally labeled panel for each molecule. We compute average precision (AP) for panels containing both label classes and report molecule-averaged results separately for binding and enzyme activity. Overall AP averages the per-molecule values across all 198 test queries. Metric definitions, tie handling, and aggregation details are provided in Appendix A.4.

Both protocols reuse the same query molecules and model scores, but assess distinct capabilities: target recovery across a broad candidate space and activity discrimination within measured panels. Together, the curated data, fixed splits, and evaluation protocols provide a common basis for developing and comparing reverse target-fishing methods without conflating missing measurements with experimental negatives.

5 Experiments

We evaluate GenFish against neural and traditional baselines, then examine false-negative competition and the biological structure of its semantic codes. A supplementary protein–code assignment control is provided in Appendix E.2.

We use the ProTargetBench training associations, 75 validation molecules, and 198 test molecules. All methods rank the same catalogue of 20,431 proteins. Comparators include four neural methods—DrugCLIP, HypSeek, LigUnity, and ConPLex—and three simple baselines: target frequency, similarity-weighted k-NN, and SEA.

The task is defined over sequence-derived protein representations. Methods whose original implementations use different protein inputs or supervision are therefore adapted to this common setting; configurations and implementation details are provided in Appendix D.

Headline neural results use five seeds and a ceiling of 22,560 updates. Checkpoints are selected lexicographically by validation R@10, R@50, and MRR; non-neural baselines use training or validation data only for their fixed statistics and hyperparameters. Panel evaluation reuses the catalogue-retrieval scores without reselection. Internal ablations use a common training recipe and three paired seeds. Statistical intervals are obtained by paired molecule bootstrap and are conditional on the fitted models.

5.1 Main Results

Table 1: **Full-catalogue retrieval.** All methods rank the same 20,431-protein catalogue for 198 held-out molecules. Neural results are means ± sample SD over five seeds; non-neural baselines report single results. Higher is better (↑).

198 queries × 20,431 proteins			
Method	R@10 ↑	R@50 ↑	MRR ↑
Target frequency	0.0151	0.1364	0.0352
Weighted k-NN	0.3483	0.4187	0.4227
SEA (Morgan)	0.3074	0.4092	0.3534
DrugCLIP	0.2959 ± 0.0113	0.3719 ± 0.0356	0.4144 ± 0.0131
HypSeek	0.2598 ± 0.0176	0.3402 ± 0.0397	0.3506 ± 0.0194
LigUnity	0.3286 ± 0.0104	0.4126 ± 0.0169	0.4313 ± 0.0058
ConPLex	0.2690 ± 0.0117	0.4650 ± 0.0226	0.3147 ± 0.0385
GenFish	$\mathbf{0.3527 \pm 0.0052}$	$\mathbf{0.5196 \pm 0.0177}$	$\mathbf{0.4631 \pm 0.0163}$

Full-catalogue retrieval. Full-catalogue retrieval asks whether a method can recover a molecule's recorded positive targets while ranking the entire 20,431-protein catalogue, including candidates with no measured association for that molecule. The results support the claim that semantic identifiers transfer sparse positive supervision across this broad candidate space. GenFish gains are largest for broader retrieval, where a query-independent popularity prior and local ligand similarity provide weaker coverage. This is consistent with the intended role of shared protein structure: improving known-target recovery without labeling unmeasured pairs as negative.

Table 2: **Measured-panel discrimination.** All methods reuse their catalogue-retrieval scores on the experimentally labeled panels. Overall AP is the molecule-averaged AP across binding and enzyme-activity queries. Higher is better (↑).

Measured-panel discrimination			
150 binding and 48 enzyme-activity molecules			
Method	Binding AP ↑	Enzyme AP ↑	Overall AP ↑
Target frequency	0.3433	0.7212	0.4349
Weighted k-NN	0.4339	0.7152	0.5021
SEA (Morgan)	0.5020	0.7686	0.5666
DrugCLIP	0.4707 ± 0.0167	0.7844 ± 0.0209	0.5468 ± 0.0097
HypSeek	0.4425 ± 0.0204	0.7902 ± 0.0327	0.5268 ± 0.0091
LigUnity	0.5000 ± 0.0189	$\mathbf{0.8197 \pm 0.0255}$	0.5775 ± 0.0146
ConPLex	0.4442 ± 0.0199	0.7035 ± 0.1182	0.5071 ± 0.0295
GenFish	$\mathbf{0.5134 \pm 0.0148}$	0.8122 ± 0.0264	$\mathbf{0.5858 \pm 0.0143}$

Measured-panel discrimination. This task ranks experimentally measured candidates for each molecule. GenFish achieves the strongest overall AP and binding AP, while LigUnity remains strongest on enzyme-activity panels, showing that catalogue recovery and measured activity discrimination reward complementary evidence.

5.2 Ablation Study

False-negative competition. We hide 41,290 known training positives while retaining at least one visible association for every molecule and training-supported target. The hidden labels are withheld from training but retained for identifying false-negative competition.

We compare standard contrastive training, oracle masking of hidden positives from negative competition, matched random masking, and GenFish trained on the same visible positives. All use fixed checkpoints after 22,560 updates and are evaluated on hidden-positive recovery and the original 198 held-out queries (Appendix E.1).

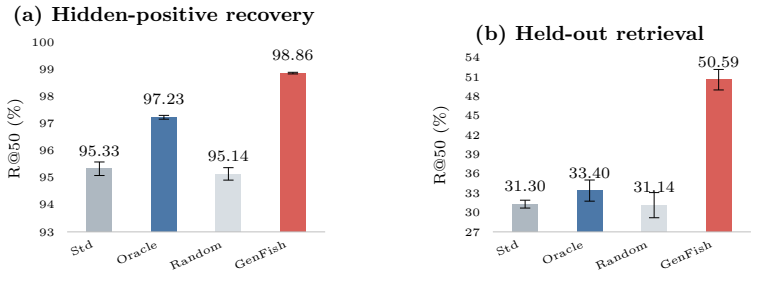


Figure 4: **False-negative competition ablation.** Hidden-positive recovery (left) and held-out retrieval (right) under standard contrastive training, oracle masking, matched random masking, and GenFish with the same visible positives. Bars show means over three seeds with sample-standard-deviation error bars.

Oracle masking increases held-out R@50 from 31.30% to 33.40% and hidden-positive recovery from 95.33% to 97.23%, confirming that false-negative competition harms contrastive training.

Under the same incomplete supervision, GenFish reaches 50.59% held-out R@50, exceeding standard contrastive training and oracle masking by 19.29 and 17.19 points, respectively. The intervention establishes that false-negative competition harms this contrastive model, while the comparison demonstrates GenFish's stronger target recovery under the same available positive supervision.

5.3 Biological Structure of the Codes

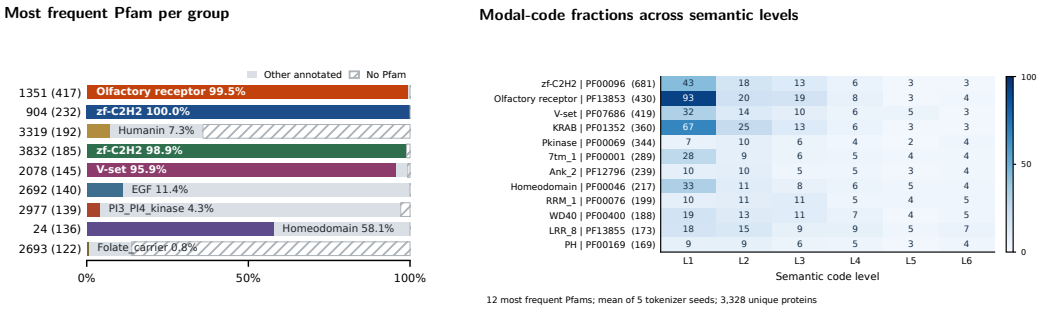


Figure 5: **Biological structure of the semantic identifiers.** Left: Pfam composition of large level-1 code groups. Right: modal-code fractions for prevalent Pfams across semantic levels. Pfam annotations are used only for this post hoc analysis and are excluded from tokenizer and retrieval training.

We use Pfam annotations, held out from tokenizer and retrieval training, to assess code–family structure. Several large groups contain coherent families; across five tokenizer seeds, $34.98\% \pm 1.34\%$ of annotated pairs sharing a level-1 code also share a Pfam, compared with 0.47% of all annotated catalogue-protein pairs (Appendix B.5).

Together, these results support GenFish and ProTargetBench as a framework for retrieval under incomplete supervision. The quantized codes retain family structure from the protein representations, suggesting that this approach can provide a useful template for other sparse scientific retrieval problems.

6 Conclusion and Future Work

GenFish combines shared protein semantic identifiers with molecule-conditioned prediction for reverse target fishing under incomplete supervision. Quantized codes let observed molecule–protein associations share supervision across candidates without treating every unmeasured pair as a negative, while ProTargetBench evaluates both full-catalogue recovery and measured-panel discrimination. GenFish improves retrieval across these settings, and controlled interventions show both the cost of false-negative competition and the value of the learned protein–code structure. These results support semantic identifiers as a practical strategy for sparse proteome-scale retrieval. The framework can be extended to other molecular modalities, biological entities, and scientific discovery problems with partially observed associations.

Ethics statement

This study uses existing biochemical data, with no new human-subject or wet-laboratory experiments. Predictions are research hypotheses, not clinical recommendations or confirmed binding. Selective measurement and assay heterogeneity limit downstream use; releases must respect source licences and preserve provenance.

Reproducibility Statement

The main text and appendices specify data sources, curation rules, evaluation protocols, model architectures, training configurations, and statistical procedures. Appendix A documents data provenance and artifact formats; Appendices B and D detail model implementations; Appendix E specifies the controlled experiments and internal ablations.

References

[1] O. J. M. Béquignon, B. J. Bongers, W. Jespers, A. P. IJzerman, B. van der Water, and G. J. P. van Westen. Papyrus: a large-scale curated dataset aimed at bioactivity predictions. *Journal of Cheminformatics*, 15(1):3, 2023. doi: 10.1186/s13321-022-00672-x.

[2] Salvatore Candido, Thomas Hayes, Alexander Derry, Roshan Rao, Zeming Lin, Robert Verkuil, Bryan Wu, Jin Sub Lee, Elise S. Bruguera, Jehan A. Keval, Mykhailo Kopylov, John E. Pak, Wesley Wu, Neil Thomas, Samson Mataraso, Alvin Hsu, Ashton C. Trotman-Grant, Kilian Fatras, Allan dos Santos Costa, Rohil Badkundri, Halil Akın, Deniz Oktay, Jonathan Deaton, Elizabeth Montabana, Hrishita Sitwala, Yue Yu, Marius Wiggert, Dylan Alexander Carlin, Anthony W. Goering, Tomasz Blazejewski, McCullen Sandora, Michael Hla, Tina Z. Jia, Leon H. Kloker, Nicholas J. Sofroniew, Masatoshi Uehara, Jassi Pannu, Sharrol Bachas, Daniel S. Liu, Tom Sercu, and Alexander Rives. Language modeling materializes a world model of protein biology, 2026. URL https://www.biorxiv.org/content/10.64898/2026.06.03.729735. bioRxiv preprint.

[3] Antoine Daina, Olivier Michielin, and Vincent Zoete. SwissTargetPrediction: updated data and new features for efficient prediction of protein targets of small molecules. *Nucleic Acids Research*, 47(W1):W357–W364, 2019. doi: 10.1093/nar/gkz382. URL https://doi.org/10.1093/nar/gkz382.

[4] Bin Feng, Zijing Liu, Hao Li, Mingjun Yang, Junjie Zou, He Cao, Yu Li, Lei Zhang, and Sheng Wang. Hierarchical affinity landscape navigation through learning a shared pocket-ligand space. *Patterns*, 2025. doi: 10.1016/j.patter.2025.101371.

[5] Bowen Gao, Bo Qiang, Haichuan Tan, Yinjun Jia, Minsi Ren, Minsi Lu, Jingjing Liu, Wei-Ying Ma, and Yanyan Lan. DrugCLIP: Contrastive protein-molecule representation learning for virtual screening. In *Advances in Neural Information Processing Systems*, volume 36, pages 44595–44614, 2023. doi: 10.52202/075280-1932. URL https://doi.org/10.52202/075280-1932.

[6] Kexin Huang, Cao Xiao, Lucas M. Glass, and Jimeng Sun. MolTrans: Molecular interaction transformer for drug–target interaction prediction. *Bioinformatics*, 37(6):830–836, 2021. doi: 10.1093/bioinformatics/btaa880. URL https://doi.org/10.1093/bioinformatics/btaa880.

[7] Michael J. Keiser, Bryan L. Roth, Blaine N. Armbruster, Paul Ernsberger, John J. Irwin, and Brian K. Shoichet. Relating protein pharmacology by ligand chemistry. *Nature Biotechnology*, 25(2):197–206, 2007. doi: 10.1038/nbt1284. URL https://doi.org/10.1038/nbt1284.

[8] Michael J. Keiser, Vincent Setola, John J. Irwin, Christian Laggner, Atheir I. Abbas, Sandra J. Hufeisen, Niels H. Jensen, Michael B. Kuijer, Roberto C. Matos, Thuy B. Tran, Ryan Whaley, Richard A. Glennon, Jérôme Hert, Kelan L. H. Thomas, Douglas D. Edwards, Brian K. Shoichet, and Bryan L. Roth. Predicting new molecular targets for known drugs. *Nature*, 462 (7270):175–181, 2009. doi: 10.1038/nature08506. URL https://doi.org/10.1038/nature08506.

[9] Sunghwan Kim, Jie Chen, Tiejun Cheng, Asta Gindulyte, Jia He, Siqian He, Qingliang Li, Benjamin A. Shoemaker, Paul A. Thiessen, Bo Yu, Leonid Zaslavsky, Jian Zhang, and Evan E. Bolton. PubChem 2025 update. *Nucleic Acids Research*, 53(D1):D1516–D1525, 2025. doi: 10.1093/nar/gkae1059. URL https://doi.org/10.1093/nar/gkae1059.

[10] Honglin Li, Zhenting Gao, Ling Kang, Hailei Zhang, Kun Yang, Kunqian Yu, Xiaomin Luo, Weiliang Zhu, Kaixian Chen, Jianhua Shen, Xicheng Wang, and Hualiang Jiang. TarFisDock: a web server for identifying drug targets with docking approach. *Nucleic Acids Research*, 34 (Web Server issue):W219–W224, 2006. doi: 10.1093/nar/gkl114. URL https://doi.org/10.1093/nar/gkl114.

[11] Shi-Wei Li, Peng-Xuan Ren, Lin Wang, Qi-Lei Han, Feng-Lei Li, Hong-Lin Li, and Fang Bai. MAI-TargetFisher: A proteome-wide drug target prediction method synergetically enhanced by artificial intelligence and physical modeling. *Acta Pharmacologica Sinica*, 46(5):1462–1475, 2025. doi: 10.1038/s41401-024-01444-z. URL https://doi.org/10.1038/s41401-024-01444-z.

[12] Tiqing Liu, Linda Hwang, Stephen K. Burley, Carmen I. Nitsche, Christopher Southan, W. Patrick Walters, and Michael K. Gilson. BindingDB in 2024: a FAIR knowledgebase of protein-small molecule binding data. *Nucleic Acids Research*, 53(D1):D1633–D1644, 2025. doi: 10.1093/nar/gkae1075. URL https://doi.org/10.1093/nar/gkae1075.

[13] Qing Luo, Sheng Wang, Hoi Yeung Li, Liangzhen Zheng, Yuguang Mu, and Jingjing Guo. Benchmarking reverse docking through AlphaFold2 human proteome. *Protein Science*, 33 (10):e5167, 2024. doi: 10.1002/pro.5167.

[14] Andreas Mayr, Günter Klambauer, Thomas Unterthiner, Marvin Steijaert, Jörg K. Wegner, Hugo Ceulemans, Djork-Arné Clevert, and Sepp Hochreiter. Large-scale comparison of machine learning methods for drug target prediction on ChEMBL. *Chemical Science*, 9(24): 5441–5451, 2018. doi: 10.1039/C8SC00148K. URL https://doi.org/10.1039/C8SC00148K.

[15] David Mendez, Anna Gaulton, A. Patrícia Bento, Jon Chambers, Marleen De Veij, Eloy Félix, María Paula Magariños, Juan F. Mosquera, Prudence Mutowo, Michał Nowotka, María Gordillo-Marañón, Fiona Hunter, Laura Junco, Grace Mugumbate, Milagros Rodriguez-Lopez, Francis Atkinson, Nicolas Bosc, Chris J. Radoux, Aldo Segura-Cabrera, Anne Hersey, and Andrew R. Leach. ChEMBL: towards direct deposition of bioassay data. *Nucleic Acids Research*, 47(D1):D930–D940, 2019. doi: 10.1093/nar/gky1075. URL https://doi.org/10.1093/nar/gky1075.

[16] Thin Nguyen, Hang Le, Thomas P. Quinn, Tri Nguyen, Thuc Duy Le, and Svetha Venkatesh. GraphDTA: predicting drug–target binding affinity with graph neural networks. *Bioinformatics*, 37(8):1140–1147, 2021. doi: 10.1093/bioinformatics/btaa921. URL https://doi.org/10.1093/bioinformatics/btaa921.

[17] Hakime Öztürk, Arzucan Özgür, and Elif Ozkirimli. DeepDTA: deep drug–target binding affinity prediction. *Bioinformatics*, 34(17):i821–i829, 2018. doi: 10.1093/bioinformatics/bty593. URL https://doi.org/10.1093/bioinformatics/bty593.

[18] Antonio Peón, Cuong C Dang, and Pedro J Ballester. How reliable are ligand-centric methods for target fishing? *Frontiers in Chemistry*, 4:15, 2016. doi: 10.3389/fchem.2016.00015. URL https://doi.org/10.3389/fchem.2016.00015.

[19] Shashank Rajput, Nikhil Mehta, Anima Singh, Raghunandan Hulikal Keshavan, Trung Vu, Lukasz Heldt, Lichan Hong, Yi Tay, Vinh Tran, Jonah Samost, Maciej Kula, Ed Chi, and Maheswaran Sathiamoorthy. Recommender systems with generative retrieval. In *Advances in Neural Information Processing Systems*, volume 36, pages 10299–10315, 2023. doi: 10.52202/075280-0452. URL https://arxiv.org/abs/2305.05065.

[20] Rohit Singh, Samuel Sledzieski, Bryan Bryson, Lenore Cowen, and Bonnie Berger. Contrastive learning in protein language space predicts interactions between drugs and protein targets. *Proceedings of the National Academy of Sciences*, 120(24), 2023. doi: 10.1073/pnas.2220778120. URL https://doi.org/10.1073/pnas.2220778120.

[21] Yi Tay, Vinh Q. Tran, Mostafa Dehghani, Jianmo Ni, Dara Bahri, Harsh Mehta, Zhen Qin, Kai Hui, Zhe Zhao, Jai Gupta, Tal Schuster, William W. Cohen, and Donald Metzler. Transformer memory as a differentiable search index. In *Advances in Neural Information Processing Systems*, volume 35, pages 21831–21843, 2022. doi: 10.52202/068431-1587. URL https://arxiv.org/abs/2202.06991.

[22] Jianhui Wang, Wenyu Zhu, Bowen Gao, Xin Hong, Ya-Qin Zhang, Wei-Ying Ma, and Yanyan Lan. Learning protein–ligand binding in hyperbolic space. In *Proceedings of the AAAI Conference on Artificial Intelligence*, volume 40, pages 1150–1158, 2026. doi: 10.1609/aaai.v40i2.37086. URL https://doi.org/10.1609/aaai.v40i2.37086.

[23] Wenjie Wang, Honghui Bao, Xinyu Lin, Jizhi Zhang, Yongqi Li, Fuli Feng, See-Kiong Ng, and Tat-Seng Chua. Learnable item tokenization for generative recommendation. In *Proceedings of the 33rd ACM International Conference on Information and Knowledge Management*, pages 2400–2409, 2024. doi: 10.1145/3627673.3679569. URL https://doi.org/10.1145/3627673.3679569.

[24] Nansu Zong, Ning Li, Andrew Wen, Victoria Ngo, Yue Yu, Ming Huang, Shaika Chowdhury, Chao Jiang, Sunyang Fu, Richard Weinshilboum, Guoqian Jiang, Lawrence Hunter, and Hongfang Liu. BETA: a comprehensive benchmark for computational drug–target prediction. *Briefings in Bioinformatics*, 23(4):bbac199, 2022. doi: 10.1093/bib/bbac199. URL https://doi.org/10.1093/bib/bbac199.

The appendices provide benchmark construction and evaluation details (Appendix A), model implementation (Appendix B), probability and scoring identities (Appendix C), external comparator configurations (Appendix D), and controlled experiments and internal ablations (Appendix E).

A Benchmark Construction, Splits, and Metrics

This appendix describes the data sources, curation rules, evaluation splits, metrics, and release contents of ProTargetBench.

A.1 Sources and Benchmark Overview

ProTargetBench combines a fixed human protein catalogue with curated bioactivity associations and experimentally measured evaluation panels. Construction standardizes molecular and protein identities, assesses measurement eligibility, applies evaluation exclusions, and aggregates the remaining evidence into training associations.

The v1 data snapshot (2026-09-10) uses ChEMBL 36, BindingDB All 202609 with assay and record sidecars, and selected reviewed PubChem panels. The PubChem component is a panel collection rather than a database-wide extraction. The human catalogue uses UniProt release 2026_03 with the query `organism_id:9606 AND reviewed:true`.

The catalogue contains 20,431 protein accessions and 20,353 distinct sequences. Distinct accessions are retained even when their sequences are identical; entries therefore do not correspond strictly to distinct genes. Of the catalogue entries, 2,303 exceed 1,022 residues and 17,564 have no positive training support. The benchmark overview in Section 4 summarizes the main benchmark counts.

The feature store contains 20,685 protein identities, including identities outside the retrieval catalogue. These additional identities do not expand the candidate set. Full-catalogue predictions follow a fixed ordering of the 20,431 candidate accessions.

A.2 Identity Standardization and Evidence Curation

Molecular identities. Molecules are standardized with RDKit 2023.09.6. The pipeline parses SMILES, rejects unparseable structures and enhanced-stereochemistry groups, removes atom maps, and applies RDKit Cleanup. Registered salts are stripped with `dontRemoveEverything=True`; unresolved multicomponent structures and nonorganic parents are excluded, and the retained parent is uncharged.

Canonical isomeric SMILES preserves stereochemistry and isotopes; tautomers are not collapsed. Molecular identifiers are SHA256 hashes of these canonical strings. Nonchiral Bemis–Murcko scaffolds are hashed separately for exclusion checks; molecules with empty scaffolds have no scaffold key. The use of nonchiral Morgan fingerprints as model inputs does not change the molecular identity policy.

Protein identities. Association-level protein identities are defined by the tuple of taxon, accession, and sequence SHA256, rather than accession alone. Primary training evidence requires resolved taxonomy, an admissible sequence, a single protein component, and a canonical construct. Sequences that conflict with the catalogue reference are not silently replaced.

Historical evaluation-panel candidates retain their frozen sequence identities when an exact canonical match is unavailable. The retrieval catalogue retains distinct accessions rather than merging them by sequence.

Activity measurements and training labels. Eligible Ki, Kd, and IC50 measurements are converted to nM using decimal arithmetic. Supported relations are $=, <, \leq, >, \geq$, with open and closed interval endpoints preserved. Nonpositive, nonfinite, malformed, and ambiguously censored range records are excluded.

A measurement provides positive evidence only if its entire admissible interval lies below 1,000 nM. Thus, "< 1000" qualifies, whereas "≤ 1000" does not. A lower bound of at least 10,000 nM provides weak-activity evidence, but is admitted as a credible negative only with verified fitted-value, experimental-bound, or validated-panel provenance. Intermediate measurements and threshold-crossing intervals remain nonbinary.

The training view used in this study contains positive associations and no admitted credible negatives. Unrecorded pairs used as competitors by a training objective are not experimentally measured negatives.

ChEMBL training records additionally require assay type B, confidence score 9, standard flag 1, no validity comment or potential-duplicate flag, and no variant sequence. Reviewed experimental contexts admit binding or enzyme activity and exclude unresolved mixed, phenotypic, or variant contexts. EC50 records may be retained in the raw evidence ledger but are not admitted as training Ki/Kd/IC50 evidence.

Duplicates and conflicts. Measurements are merged across sources only when they share the original assay identity, standardized molecule, protein identity, endpoint, experimental context, and interval bounds. Otherwise, they remain source-local records.

Within a common endpoint and context, positive evidence combined with weak or credible-negative evidence is flagged as conflicting. Strong measurements that conflict with inactive-text assertions are also flagged rather than averaged. Incomparable endpoints are not combined into a single affinity value.

Evaluation exclusions are applied before evidence is reaggregated. Admitted molecule–protein identity pairs are then deduplicated so that repeated measurements do not multiply their contribution to the training loss.

A.3 Evaluation Panels and Split Construction

Panel sources and labels. Evaluation queries retain their frozen source-specific experimental labels. Binding and enzyme panels are evaluated separately. The resource descriptions [9, 12, 15] document the databases; they do not replace the original assay evidence supporting each retained label.

Panel labels follow source-specific criteria rather than a universal threshold. Positive labels generally require eligible sub-micromolar measurements with admissible primary evidence. Negative labels require source-supported evidence, such as an explicit lower bound of at least $10\,\mu$M or a documented inactive call satisfying the applicable counter-screen criteria. Conflicts between strong activity measurements and primary inactive calls are excluded rather than averaged.

Dose-response sources require complete dose series and admissible curve classes. Exact assay identifiers, curve-class and response cutoffs, counter-screen rules, and reviewed BindingDB or patent-table references are specified in the release manifest. These source-specific predicates are required to reproduce the panel labels; the general thresholds above do not replace them.

Frozen evaluation split. The evaluation split, referred to as *Anchor* in the data artifacts, contains 75 validation molecules and 198 test molecules. The validation set comprises 53 binding and 22 enzyme queries; the test set comprises 150 binding and 48 enzyme queries.

The validation and test query payloads retain their frozen identities, labels, and source provenance.

Catalogue size, the number of training-supported proteins, and the number of experimentally measured panel targets describe different aspects of the benchmark and are reported separately.

Training exclusions. Before constructing the final training view, the builder excludes evaluation molecules, their nonempty scaffold keys, the frozen held-out scaffold list, and historical molecule and pair exclusion lists. Evaluated DOI, PMID, and assay aliases are expanded through the source-identity graph so that reviewed evidence exclusions apply across linked sources and species. Previously identified conflicting pairs remain flagged.

These operations filter the training evidence while preserving the frozen validation and test queries. They should not be interpreted as establishing additional pairwise scaffold-disjointness guarantees between validation and test beyond the recorded split policy.

Validation-based selection. Hyperparameters and model configurations are selected using validation data. Learning-rate selection uses three-seed mean validation R@10, with ties broken by R@50 and then MRR. Both test protocols use the resulting catalogue-selected checkpoints; measured-panel test AP is not used for checkpoint reselection.

Derived panels retain their parent-source provenance and are not treated as newly collected external data.

A.4 Metrics and Statistical Reporting

Full-catalogue retrieval. Let $\mathcal{P}_x^+$ denote the set of recorded positive catalogue targets for query molecule x, and let $\mathrm{TopK}(x)$ denote the first K proteins in its ranked catalogue. Recall is

$$\mathrm{R@K}(x) = \frac{|\mathcal{P}_x^+ \cap \mathrm{TopK}(x)|}{|\mathcal{P}_x^+|}. \tag{8}$$

The reciprocal rank is determined by the highest-ranked recorded positive:

$$\mathrm{RR}(x) = \frac{1}{\min_{p \in \mathcal{P}_x^+} \mathrm{rank}_x(p)}. \tag{9}$$

We report molecule-macro R@10, R@50, and MRR by averaging the corresponding query-level values over the evaluation molecules. These metrics assess the recovery of recorded positives; they do not establish that higher-ranked unmeasured associations are biologically inactive.

Measured-panel discrimination. Average precision is calculated using groups of equal prediction scores:

$$\mathrm{AP}(x) = \sum_t (R_t - R_{t-1})\,\mathrm{Precision}_t, \tag{10}$$

where t indexes successive score thresholds and R_t is recall among the panel's experimentally labeled positives. Processing tied scores as a group avoids arbitrary ordering within ties.

Where AUROC is computed, it is the fraction of positive–negative comparisons won by the positive, with half credit for a tie. Scores are averaged over queries within a molecule when needed, and then over molecules.

We report binding-tier and enzyme-tier macro AP separately. Overall AP is

$$\mathrm{AP}_{\mathrm{overall}} = \frac{150\ \mathrm{AP}_{\mathrm{binding}} + 48\ \mathrm{AP}_{\mathrm{enzyme}}}{198}. \tag{11}$$

Because the tiers are disjoint, this equals the mean of the 198 molecule-level AP values. It is neither AP computed from pooled predictions nor an average weighted by panel size.

For neural methods, Overall AP is computed separately for each seed before calculating its mean and sample standard deviation, preserving covariance between the two tiers. This descriptive aggregate was added after inspection of tier-specific results, without changing model fitting or checkpoint selection.

Seeds and uncertainty. The initial catalogue experiments use seeds 13, 37, and 73. Seeds 101 and 211 are added as confirmatory runs for the headline comparison, using fresh supervised initializations and the same model recipes. For GenFish, the tokenizer is also fitted afresh under the same 500-epoch feature-reconstruction protocol. No replication seed is omitted.

Neural headline results report five-seed means and sample standard deviations, with denominator $n - 1$. Internal controlled-study intervals use 10,000 paired molecule-bootstrap resamples. The low-similarity comparisons are specified in Appendix D.7. Bootstrap intervals quantify query-sampling uncertainty conditional on the fitted models, rather than the full uncertainty from training or experimental-source sampling.

A.5 Release Contents and Provenance

Versioned manifests, policies, verification logs, and source/hash indices identify the data views and evaluation splits. The staged derived release contains catalogue sequences, standardized molecular structures, training evidence groups, query labels, exclusion policies, a loader, and initial predictions. It also includes historical material outside the current evaluation.

The loader verifies molecular structure hashes under the identity policy above. Protein identities follow the taxon/accession/sequence-hash policy, while catalogue file order defines the canonical candidate ordering and prediction records identify candidates by UniProt accession.

The staged Anchor prediction files contain scored top-200 lists and the full-catalogue rank of every recorded positive, allowing exact recomputation of R@10, R@50, and MRR. All twelve staged method/seed files reproduce their originating metrics within numerical precision, but do not cover every manuscript result.

Raw source-ledger measurements are not redistributed. Retained `evidence_id` and `source_molecule_id` fields support label-level audit against ChEMBL 36 and BindingDB All 202609. The derived release supports inspection of the frozen benchmark views but does not, by itself, establish independent reconstruction of the primary-source splits from scratch.

B Model Implementation and Training

B.1 Protein Features and Sequence Pooling

We extract frozen 1,152-dimensional protein features using ESMC-600M [2]. Sequences are divided into nonoverlapping windows of at most 1,022 residues. Residue representations exclude special tokens and are averaged across the complete sequence.

For a sequence of length n_p, let $B_p = \lceil n_p/1022 \rceil$ be the number of windows, $m_{p,b}$ the length of window b, and $H_{p,b,t}$ the representation of its tth residue. The pooled feature is

$$\widetilde{h}_p = \sum_{b=1}^{B_p} \frac{m_{p,b}}{n_p} \left(\frac{1}{m_{p,b}} \sum_{t=1}^{m_{p,b}} H_{p,b,t} \right). \tag{12}$$

This gives equal weight to every residue while covering the full sequence. Residues are encoded within their respective windows, without cross-window context.

The pooled features are standardized coordinate-wise using the fitting population's means and sample standard deviations, with standard deviations clamped below at 10^{-6}. We denote the standardized feature by h_p. Feature standardization and tokenizer fitting use all 20,685 core protein identities, including the 20,431 catalogue entries. Additional feature-store identities are not retrieval candidates.

B.2 Tokenizer Construction and Training

Residual quantization. An encoder E maps h_p to a latent representation $z_p \in \mathbb{R}^{32}$. At level ℓ, a codebook $\{e_{\ell,k}\}_{k=1}^{K_\ell}$ quantizes the current residual:

$$r_0 = z_p, \qquad c_\ell(p) = \arg\min_k \|r_{\ell-1} - e_{\ell,k}\|_2^2, \qquad q_\ell = e_{\ell,c_\ell(p)}. \tag{13}$$

Nearest-vector ties are resolved by the lowest code index. The six codebook sizes are $(4096, 32, 128, 128, 256, 128)$.

Each selected vector is subtracted from the residual. The sum of selected vectors is passed through a decoder to reconstruct the standardized protein feature. The tokenizer uses hidden width 256 and latent dimension 32.

Objective and gradient estimator. The straight-through estimator and reconstruction are

$$\widetilde{q}_\ell = r_{\ell-1} + \mathrm{sg}(q_\ell - r_{\ell-1}), \qquad r_\ell = r_{\ell-1} - \widetilde{q}_\ell, \qquad \widehat{h}_p = D\left(\sum_{\ell=1}^{6} \widetilde{q}_\ell\right). \tag{14}$$

The training objective is

$$\mathcal{L}_{\mathrm{tok}} = \mathrm{MSE}(\widehat{h}_p, h_p) + \sum_{\ell=1}^{6} \left[\mathrm{MSE}(\mathrm{sg}(q_\ell), r_{\ell-1}) + 0.25\ \mathrm{MSE}(q_\ell, \mathrm{sg}(r_{\ell-1}))\right], \tag{15}$$

where sg stops gradients and MSE averages squared elementwise errors. The tokenizer is trained for 500 epochs using Adam with learning rate 10^{-3}, then frozen for molecular predictor training. Its objective uses protein features rather than interaction labels.

For the displayed estimator, treating discrete assignments as fixed,

$$\frac{\partial \widetilde{q}_\ell}{\partial r_{\ell-1}} = I, \qquad \frac{\partial r_\ell}{\partial r_{\ell-1}} = 0. \tag{16}$$

Consequently, later levels do not propagate gradients to earlier levels through the residual path. Reconstruction gradients reach the encoder through the first straight-through path, while the explicit codebook term updates the code vectors.

Collision-resolving suffix. Proteins are grouped by their complete six-code semantic tuple. Within each group, consecutive suffix integers starting at zero are assigned in the fixed protein-feature row order. The suffix vocabulary size equals the largest collision-group size; singleton groups receive suffix zero.

The suffix has no reconstruction vector. It is predicted by an independent head and participates in both code cross-entropy and retrieval scoring. For the internal experiments with seeds 13, 37, and 73, its vocabulary sizes are 11, 10, and 8, respectively. This assignment is fixed for the catalogue; extending the catalogue may require updating the suffix assignment and prediction vocabulary.

B.3 Molecular Predictor and Conditional Interaction

Shared predictor. Molecules are represented by 2,048-bit Morgan fingerprints with radius two. A shared molecular network uses two 512-wide ReLU layers with dropout 0.1, followed by seven code-prediction heads. The first semantic code and the suffix are predicted without predecessor conditioning. Five interaction modules modify the logits at semantic levels 2–6.

Conditional modules. Each module uses interaction width 16. For a fixed query x, the matrix of logit corrections across predecessor and current codes is

$$\Delta_j(x) = \bar{U}_j \operatorname{diag}(g_j(x)) V_j^\top, \qquad \operatorname{rank}(\Delta_j(x)) \le 16. \tag{17}$$

Here $\bar{U}_j$ contains row-normalized predecessor embeddings, with norms clamped below at 10^{-12}. The rank bound applies to the logit correction, not necessarily to the resulting softmax probability matrix.

The five modules add

$$\sum_{j=2}^{6} [16(K_{j-1} + K_j) + 16 \cdot 512 + 16] = 126{,}032 \tag{18}$$

parameters to the base predictor.

The matrices U_j and V_j are initialized from standard normal distributions. Gate weights and biases are initialized to zero, so the conditional model initially reproduces the base logits. Additional tensors use an independent CPU random number generator seeded with the training seed plus 1,000,003, preserving the base-model initialization and dropout random-number state.

Training and scoring. All variants sum seven equally weighted code cross-entropies during training and the corresponding log-probabilities during retrieval. Conditional distributions are normalized over the full vocabulary at each level, without a reachable-code mask. Candidates are not excluded because their codes lack positive training support.

B.4 Training Configurations

The internal comparisons use the same molecular features, frozen tokenizer for each seed, and positive training associations. Optimization uses Adam with learning rate 10^{-4}, zero weight decay, $\beta = (0.9, 0.999)$, $\epsilon = 10^{-8}$, and batch size up to 4,096.

Validation is performed every 94 updates. Checkpoints are selected by validation R@10, breaking ties by R@50, then MRR, and retaining the earliest checkpoint for remaining ties. Appendix E reports the controlled positive-hiding experiment.

These fixed internal settings are distinct from the validation-selected headline configurations, which are documented in Appendix D. Training used NVIDIA A100 40 GB GPUs.

B.5 Pfam Annotation and Code-Structure Analysis

Annotation population. We use UniProt Pfam cross-references for the frozen catalogue, retrieved on 10 September 2026. Each accession–Pfam membership is counted once; domain positions and repeated-domain copy counts are not available in this analysis.

Of the 20,431 catalogue proteins, 19,457 (95.23%) have at least one Pfam annotation, 974 have none, and 8,389 have multiple distinct annotations. The analysis retains all 8,953 observed Pfam entries and 34,956 memberships. Missing cross-references are not interpreted as an absence of

domains. Pfam display names are obtained through the InterPro API without changing the frozen memberships. Pfam annotations are not used to train the tokenizer or retrieval model.

Composition of displayed groups. For each displayed code group, Figure 5 identifies its most frequent Pfam, with Pfam-ID order breaking frequency ties. Proteins are divided into three disjoint categories: those carrying this Pfam, those carrying other Pfams but not this Pfam, and those without annotations.

All group members are included. Assigning a protein to a display category does not remove any of its additional Pfam memberships from the statistical analysis.

Within-Pfam code concentration. For tokenizer seed s, semantic level j, Pfam f, and code c, let n_{sjfc} count proteins annotated with f and assigned to c. The concentration of f at this level is

$$C_{sjf} = \frac{\max_c n_{sjfc}}{n_f}, \qquad n_f = \sum_c n_{sjfc}. \tag{19}$$

Figure 5 reports five-seed mean concentrations for the twelve most prevalent Pfams, with Pfam-ID order breaking frequency ties. These rows cover 3,328 unique proteins. Because proteins may carry multiple Pfams, row populations overlap and should not be summed.

Concentration measures how strongly a Pfam is assigned to a single code, rather than a one-to-one correspondence between codes and families. Codebook sizes differ across levels, so concentration values do not provide a capacity-controlled ranking of semantic quality.

Protein-pair correspondence. Let A_p be the set of Pfams assigned to protein p, and let $\mathcal{A}$ contain catalogue proteins with at least one annotation. For seed s and level j, we calculate

$$R_{sj} = \frac{\sum_{\substack{p<q \\ p,q\in\mathcal{A}}} \mathbf{1}[c_{sj}(p) = c_{sj}(q)]\mathbf{1}[A_p \cap A_q \neq \varnothing]}{\sum_{\substack{p<q \\ p,q\in\mathcal{A}}} \mathbf{1}[c_{sj}(p) = c_{sj}(q)]}. \tag{20}$$

Each unordered protein pair contributes once, irrespective of the number of shared Pfams. The catalogue reference is the corresponding fraction across all annotated protein pairs, without restricting them to a shared code: 0.4742%. This is an observed background fraction, not a simulated null distribution.

Across tokenizer seeds 13, 37, 73, 101, and 211, the first-level statistic is $34.98\% \pm 1.34\%$ (mean $\pm$ sample SD). Figure 6 reports all semantic levels and the collision suffix. Differences in codebook sizes, group sizes, and eligible pair populations should be considered when comparing levels. These statistics assess annotation correspondence; the retrieval contribution of protein–code assignments is evaluated separately in Appendix E.2.

C Code Probabilities and Exact Catalogue Scoring

Let $c(p)$ denote the complete seven-code identifier of protein p, and let $Q(c \mid x)$ denote the code distribution conditioned on molecule x. The tokenizer and identifier assignments remain fixed during molecular predictor training.

C.1 Identifier and Probability Definitions

The six semantic codes may be shared by multiple proteins. A fixed suffix distinguishes identities within each collision group, making complete identifiers unique within the encoded protein universe.

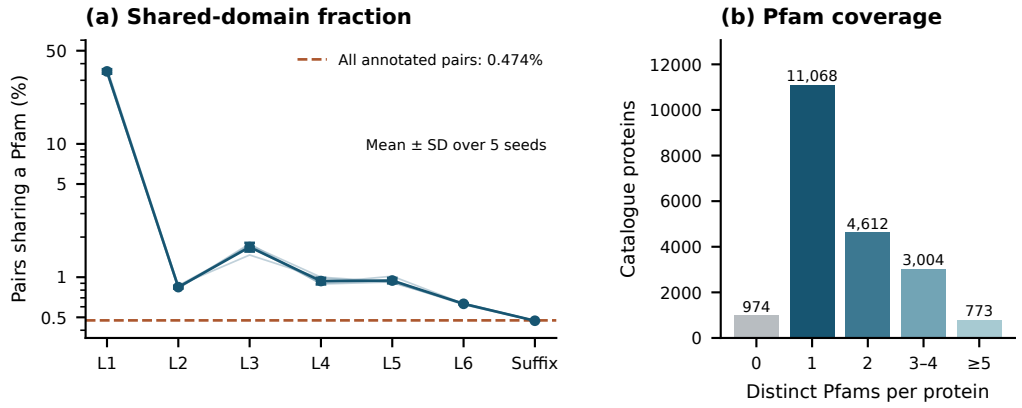


Figure 6: **Pfam correspondence across code levels and catalogue annotation coverage.** (a) Fraction of annotated protein pairs sharing a code that also share at least one Pfam. Thin lines show five tokenizer seeds; markers and error bars indicate their mean and sample standard deviation. The vertical axis is logarithmic. The dashed line shows the fraction among all annotated catalogue pairs. The suffix resolves identifier collisions and is not a semantic level. (b) Catalogue protein counts by number of distinct Pfam annotations; zero indicates missing cross-references.

Let $\mathcal{P}$ be the candidate catalogue and $\mathcal{C} = \prod_{j=1}^{7}\{0, \ldots, K_j - 1\}$ the identifier space. GenFish defines

$$Q(c \mid x) = \prod_{j=1}^{7} P_j(c_j \mid x, c_{j-1}), \qquad c_0 = \varnothing, \tag{21}$$

where levels 1 and 7 omit predecessor conditioning. Each factor is normalized over its full vocabulary, so Q sums to one over $\mathcal{C}$.

C.2 Training Objective and Exact Scoring

Summing seven equally weighted code cross-entropies gives the positive-pair loss $-\log Q(c(p) \mid x)$. The objective uses recorded positives without assigning experimental negative labels to unmeasured pairs. At retrieval time, each candidate is evaluated along its stored identifier; the sum of normalized code log-probabilities is the exact log-likelihood in Eq. 21. Scoring requires neither a generated prefix nor knowledge of the query's true target.

D External Comparators and Training Configurations

We compare GenFish with four neural methods and three simple baselines using the same retained positive associations and candidate catalogue. DrugCLIP, HypSeek, and LigUnity are adapted to frozen ESMC-600M protein features and Morgan-2048 molecular fingerprints. ConPLex retains its native ProtBERT-based projection architecture.

Prepared binding sites are unavailable for most catalogue proteins, so pocket-based encoders are replaced with sequence-feature towers. The adaptations below retain selected components of the published methods while specifying changes to inputs, architecture, and objectives. The comparisons therefore evaluate complete training configurations rather than scoring functions alone.

D.1 DrugCLIP

Our DrugCLIP adaptation uses dual encoders, L_2-normalized embeddings, inner-product scoring, and a bidirectional multi-positive contrastive objective, following the retrieval formulation of Gao et al. [5]. The protein tower operates on frozen ESMC-600M features, while the molecular tower uses Morgan-2048 fingerprints. Architecture and optimization settings are given in Appendix D.6.

D.2 HypSeek

The HypSeek adaptation uses a hyperbolic representation based on Wang et al. [22]. With curvature fixed to one, tower outputs v are lifted as

$$\exp_0(v) = \left(\cosh \|v\|, \frac{\sinh \|v\|}{\|v\|} v\right), \tag{22}$$

using the continuous limit at $v = 0$. Retrieval uses the temperature-scaled inner product of the spatial components. Tangent norms are capped so that spatial norms remain within $[0, 1]$.

The sequence towers and contrastive objective follow the DrugCLIP adaptation. The adapted objective omits the affinity-ordered Plackett–Luce and entailment-cone terms. The binary training view does not provide within-assay affinity orderings for the affinity-ordered component.

D.3 LigUnity

The LigUnity adaptation retains cosine scoring, bidirectional in-batch contrastive training, and ligand-to-target and target-to-target refinement branches [4]. Ligand-to-target aggregation averages molecular tower representations of each target's training ligands. Two-hop target aggregation supplies neighboring ligand profiles, including for targets without direct training support.

Pocket encoders are replaced with sequence towers. Each target connects to its 16 nearest training-supported neighbors by frozen protein-feature cosine similarity, replacing pocket-alignment edges. Aggregation uses uniform averaging instead of learned attention, and the affinity-ordered pharmacophore-ranking loss is omitted.

Refinement gates are initialized to zero. Shared submodules are initialized before the additional branches to preserve their initial parameters across matched configurations.

D.4 ConPLex

We retain the official SimpleCoembedding architecture of Singh et al. [20]. Morgan-2048 molecular inputs and frozen ProtBERT-1024 protein features each pass through a single linear projection followed by ReLU, producing 1,024-dimensional representations scored by cosine similarity. Both projections are initialized afresh, without a supervised interaction checkpoint.

ProtBERT features use mean pooling excluding special tokens. Sequences are divided into nonoverlapping windows of at most 1,022 residues, with window representations aggregated by residue count. Protein identities and full-sequence hashes are checked against the catalogue. Unlike the other neural methods, ConPLex retains ProtBERT rather than ESMC features.

Training uses binary cross-entropy on the nonnegative cosine score with numerical clamping. The external DUDE decoy-contrastive stage is omitted. Each update contains 4,096 positive pairs and an equal number of sampled unknown pairs. The unknown-pair sample is fixed for each seed, excludes each molecule's known training positives, and draws targets only from the training-supported set. Validation and test labels are not used in sampling. These unknown pairs provide negative training labels but are not experimentally verified negatives.

Optimization uses AdamW with weight decay 0.01 and cosine warm restarts every ten positive-data passes. The 22,560-update ceiling corresponds to 242.39 positive-data passes, approximately 1% more than the 240 passes of the ESMC-based methods. Update counts are controlled, but pair evaluations and computational cost are not identical.

We search learning rates $\{5 \times 10^{-5}, 10^{-4}, 2 \times 10^{-4}\}$ using seeds 13, 37, and 73. Validation selects 10^{-4}; seeds 101 and 211 use this setting without retuning. All five selected checkpoints are reused for measured-panel and similarity-stratified evaluation.

Cached matrix scores agree with sampled official pairwise forward scores within 4.2×10^{-6} absolute error. The scorer retains the official zero-norm convention for queries whose ReLU projections are zero. All seeds are included, including the variation in enzyme AP (0.7035 ± 0.1182).

D.5 Simple Baselines

All three baselines use the same deduplicated training-positive associations and frozen candidate catalogue.

Target frequency. Each protein is scored by its number of distinct training ligands. This ranking is independent of the query molecule.

Weighted k-NN. For each query, we retrieve the globally nearest k training molecules using Tanimoto similarity on binary radius-two Morgan-2048 fingerprints. A target's score is the sum of similarities from neighbors carrying that target label, without target-frequency correction. Targets receiving no votes have score zero.

Validation selects $k = 50$ from $\{1, 3, 5, 10, 20, 50, 100, 200\}$ by R@10, then R@50 and MRR; remaining ties favor smaller k. Neighbor ties use molecular identifier order, and target-score ties use the frozen catalogue order.

SEA. SEA (Morgan) reimplements the similarity ensemble formulation [7, 8]. For each target, the raw score s sums query-to-training-ligand Tanimoto similarities strictly above 0.3. It is standardized against a training-only background:

$$z = \frac{s - an}{bn^c}, \tag{23}$$

where n is the target's training-ligand count and the fitted constants are $a = 0.0006492743$, $b = 0.01237402$, and $c = 0.6397422$. Targets are ranked by the negative logarithm of the Gumbel-tail probability. Targets without training ligands receive score zero.

The similarity threshold follows the authors' ECFP4 configuration, while fingerprints and background fitting use the present benchmark. Background fitting uses 512 training queries, 16 random subsets per query, and 20 logarithmically spaced set sizes. A separate set of 128 training queries is used to diagnose calibration without tuning. The tail probabilities describe the approximate similarity background, not biological binding probabilities.

The same fixed baseline scores are used for full-catalogue retrieval, measured-panel AP, and similarity-stratified analysis.

D.6 Headline Neural Configurations and Selection

All headline neural methods use Morgan-2048 molecular inputs and the same 381,225 positive training associations. DrugCLIP, HypSeek, LigUnity, and GenFish use frozen ESMC-600M protein features; ConPLex uses the architecture and inputs specified above.

For the ESMC-based methods, the shared molecular trunk has two 512-wide ReLU layers. The three adapted comparators project molecular representations to 256 dimensions and use a protein tower with one 512-wide hidden layer and a 256-dimensional output. GenFish uses seven code heads and the conditional modules in Appendix B.3. LigUnity additionally uses the refinement branches described above.

The four ESMC-based methods use batches of up to 4,096 positive associations, retain the final partial batch, and train for at most 22,560 updates. Validation is performed every 94 updates. Weight decay is zero, with optimizer parameters $\beta = (0.9, 0.999)$ and $\epsilon = 10^{-8}$.

The contrastive objectives average forward and reverse multi-positive log-sum-exp losses, using known training positives in the batch and up to 2,048 additional training-supported candidates. GenFish sums seven equally weighted code cross-entropies and does not use a contrastive temperature. Selected configurations are listed in Table 3.

Configurations are selected using three-seed mean validation performance over seeds 13, 37, and 73. Selection prioritizes R@10, then R@50, then MRR, with configuration identifier breaking remaining ties. Seeds 101 and 211 are subsequently trained without retuning.

Within each run, checkpoints follow the same validation metric ordering, with the earliest checkpoint retained for exact ties. Measured-panel and similarity-stratified evaluations reuse these catalogue-selected checkpoints. Selected update counts are provided in the supplementary CSV; no headline run selected the final update ceiling.

D.7 Similarity-Stratified Retrieval

We stratify the 198 test molecules by their maximum Morgan-fingerprint Tanimoto similarity to a training ligand. The groups contain 43 molecules below 0.4, 79 in $[0.4, 0.6)$, and 76 at or above 0.6. Table 4 reports all eight methods. Predictions and checkpoints are reused without refitting or reselection.

For the below-0.4 group, we compare GenFish with LigUnity, the strongest overall neural comparator on R@10 and MRR. The mean differences are $+0.0059$ for R@10, $+0.0096$ for R@50, and $+0.0252$ for MRR. The corresponding paired intervals are $[-0.0182, +0.0306]$, $[-0.0650, +0.0812]$, and $[-0.0039, +0.0578]$.

GenFish leads in two of five seed pairs for R@10, three for R@50, and all five for MRR. All three intervals include zero, so the higher means do not establish a statistically resolved ordering in this small group.

D.8 Statistical Comparisons

All reported comparison intervals use 10,000 paired molecule-bootstrap resamples. Seed-specific metric values are first averaged for each molecule; the same sampled molecule indices are then applied to both methods.

The low-similarity comparisons with LigUnity use pointwise 95% percentile intervals, defined by the 2.5th and 97.5th bootstrap percentiles. Seed-wise win counts are reported separately.

The two prespecified R@50 comparisons against target frequency and weighted k-NN use Bonferroni-adjusted intervals targeting 95% family-wise coverage. Each interval uses the 1.25th and 98.75th bootstrap percentiles. The separately conducted SEA comparison uses a pointwise 95% interval without multiplicity adjustment.

These intervals quantify query-sampling uncertainty conditional on the fitted models and baseline configurations; they do not incorporate training-seed uncertainty.

Table 3: Validation-selected headline configurations. Temperature applies only to contrastive objectives. Parameter counts refer to the trainable predictors and exclude frozen protein feature extractors.

Method	Learning rate	Dropout	Temperature	Parameters	Optimizer
DrugCLIP (adapted)	5×10^{-5}	0.1	0.03	2,164,736	AdamW
HypSeek (adapted)	10^{-4}	0.1	0.03	2,164,736	AdamW
LigUnity (adapted)	5×10^{-5}	0.1	0.07	4,525,570	AdamW
ConPLex (no-DUDE)	10^{-4}	0.0	–	3,147,776	AdamW
GenFish	10^{-4}	0.0	–	3,887,864	Adam

Table 4: Full-catalogue retrieval stratified by maximum training-ligand Tanimoto similarity. All methods reuse the scores in Table 1, without refitting. Neural entries report five-seed means ± sample SD; other entries are single results. Higher is better for all metrics (↑); bold marks the highest mean within each metric and similarity group.

Retrieval by training-ligand similarity

Maximum Morgan-fingerprint Tanimoto similarity; median 0.511

Method	$[0, 0.4)$, $n = 43$	$[0.4, 0.6)$, $n = 79$	$[0.6, 1]$, $n = 76$
R@10 ↑			
Target frequency	0.0000	0.0248	0.0135
Weighted k-NN	0.0777	**0.4332**	0.4130
SEA (Morgan)	0.0667	0.4059	0.3411
DrugCLIP (adapted)	0.0527 ± 0.0066	0.3724 ± 0.0149	0.3539 ± 0.0199
HypSeek (adapted)	0.0342 ± 0.0141	0.3312 ± 0.0197	0.3133 ± 0.0339
LigUnity (adapted)	0.0847 ± 0.0153	0.3910 ± 0.0170	0.4017 ± 0.0136
ConPLex (no-DUDE)	0.0514 ± 0.0151	0.3562 ± 0.0158	0.3016 ± 0.0363
GenFish	$\mathbf{0.0905 \pm 0.0152}$	0.4143 ± 0.0095	$\mathbf{0.4371 \pm 0.0141}$
R@50 ↑			
Target frequency	0.1197	0.1308	0.1516
Weighted k-NN	0.0874	0.4866	0.5354
SEA (Morgan)	0.0667	0.4777	0.5318
DrugCLIP (adapted)	0.0815 ± 0.0177	0.4394 ± 0.0403	0.4662 ± 0.0551
HypSeek (adapted)	0.0546 ± 0.0150	0.3961 ± 0.0300	0.4437 ± 0.0759
LigUnity (adapted)	0.1400 ± 0.0414	0.4560 ± 0.0209	0.5217 ± 0.0228
ConPLex (no-DUDE)	0.1185 ± 0.0121	0.5237 ± 0.0133	0.5999 ± 0.0444
GenFish	$\mathbf{0.1496 \pm 0.0249}$	$\mathbf{0.5503 \pm 0.0098}$	$\mathbf{0.6971 \pm 0.0274}$
MRR ↑			
Target frequency	0.0091	0.0303	0.0551
Weighted k-NN	0.0972	0.4584	0.5698
SEA (Morgan)	0.0625	0.4188	0.4499
DrugCLIP (adapted)	0.0691 ± 0.0187	0.4192 ± 0.0090	0.6048 ± 0.0293
HypSeek (adapted)	0.0432 ± 0.0179	0.3617 ± 0.0317	0.5130 ± 0.0396
LigUnity (adapted)	0.0898 ± 0.0144	0.4346 ± 0.0116	0.6211 ± 0.0118
ConPLex (no-DUDE)	0.0560 ± 0.0142	0.3565 ± 0.0702	0.4176 ± 0.0287
GenFish	$\mathbf{0.1150 \pm 0.0179}$	$\mathbf{0.4846 \pm 0.0187}$	$\mathbf{0.6377 \pm 0.0350}$

E Controlled Experiments

This appendix gives the full protocol for the false-negative intervention and the protein–code assignment permutation; the former is summarized in the main text, while the latter is reported here as a supplementary control.

E.1 Controlled Negative-Supervision Intervention

Hidden-positive construction. Using split seed 20260920, we reserve at least one positive association per molecule and originally supported protein from the 381,225 training positives. Among the remaining 82,581 eligible pairs whose targets belong to the evaluation catalogue, we hide 41,290

pairs (half, rounded down). This leaves 339,935 visible positives while preserving molecule and target training support.

The hidden set covers 31,895 training-seen molecules and 1,138 targets. It represents 10.83% of all training associations; the 50% hiding fraction applies only to the eligible subset. Validation and test labels remain unchanged.

Contrastive interventions. Standard training uses the visible positives with the adapted DrugCLIP model's bidirectional multi-positive contrastive loss.

Oracle masking removes hidden-positive cells from the forward and active reverse competition denominators without restoring their positive labels. Visible-positive numerators, reverse-anchor eligibility, candidate sets, and loss-averaging denominators remain unchanged.

Matched random masking removes the same number of cells per molecule and reverse-active status, excluding all originally known positives, including the hidden ones. It preferentially matches target-support bins of 1–4, 5–19, 20–99, 100–499, and at least 500 training associations. When a bin lacks eligible cells, selection falls back to the nearest available log-support degree with the same reverse-active status.

Fixed pair priorities make the batch-conditional selection deterministic. Masking does not introduce replacement candidates. Oracle masking uses withheld ground truth to remove false-negative competition, while random masking controls for a matched reduction in competition.

Matched training. The three contrastive treatments and GenFish use seeds 13, 37, and 73, 4,096-positive batches, matched positive-example schedules, and 22,560 updates. The contrastive treatments additionally share initialization, candidate schedules, and dropout streams.

Previously selected model-specific settings remain fixed. DrugCLIP uses AdamW with learning rate 5×10^{-5}, dropout 0.1, and temperature 0.03. GenFish uses Adam with learning rate 10^{-4}, dropout 0, and its frozen tokenizer. Both use zero weight decay. Architecture and headline configurations are described in Appendices B.3 and D.

All treatments are evaluated using their final checkpoints, without checkpoint selection on hidden-positive or test performance. The GenFish extension was specified after the contrastive results and before its training runs.

Evaluation endpoints. Both endpoints use molecule-macro R@50 over the same 20,431-protein catalogue.

Hidden-positive recovery evaluates the withheld targets of the 31,895 affected training-seen molecules. Visible positives remain in the ranked candidate catalogue but are not counted as hidden positives. Held-out retrieval evaluates the original 198 test molecules using their unchanged positive labels.

Figure 4 reports means and sample standard deviations over three seeds.

Uncertainty and supplementary effects. Effect intervals use seed-averaged per-molecule metric values and 10,000 paired molecule-bootstrap resamples. Bonferroni-adjusted intervals target 95% family-wise coverage separately for two families of four contrasts: oracle versus standard and random masking at both endpoints; and GenFish versus standard and oracle-masked training at both endpoints. The intervals condition on the fitted models and the fixed hidden-positive split.

Section 5.2 reports the held-out oracle effects. For hidden-positive recovery, oracle masking improves over standard and random-masked training by 1.91 and 2.09 percentage points, with adjusted intervals $[1.78, 2.04]$ and $[1.95, 2.23]$, respectively. All four oracle contrasts are positive in every seed.

For held-out retrieval, GenFish exceeds standard and oracle-masked contrastive training by 19.29 and 17.19 percentage points, with adjusted intervals $[15.13, 23.79]$ and $[13.00, 21.65]$, respectively.

E.2 Protein–Code Assignment Permutation

The frequency-matched null permutes complete seven-code tuples only between proteins with equal training-association degree. Thus the relation-weighted frequency of every code value is unchanged at every level, while the assignment of tuples to proteins is altered. Across the three tokenizer seeds, 97.4–97.7% of tuples move. We retrain Independent, Factorized, and GenFish under the original and permuted assignments using the same 120-epoch recipe, seeds 13, 37, and 73, and fixed 20,431-protein catalogue. Molecule–protein labels, model architecture, optimization schedule, and evaluation protocol are otherwise unchanged.

Under this controlled recipe, the original assignment exceeds the frequency-matched null by 2.62 percentage points in R@10 and 5.56 points in R@50, with the original assignment preferred for all three seeds. The control therefore tests whether the protein–code correspondence carries information beyond code frequency. It is a retrieval control rather than a claim that the quantizer alone causes all observed biological structure; the independent Pfam analysis in Section 5.3 provides complementary evidence.